Scientific Research Publishing

Journal of Materials Science and Chemical Engineering, 2024, 12, 83-91
https://www.scirp.org/journal/msce
ISSN Online: 2327-6053
ISSN Print: 2327-6045

Biomimetic Infiltrating Surface Construction Based on Micro and Nano Structures

Zhicheng Zhou[#], Jiayu Li[*#], Sisi Lu[†], Quanying Lin[‡]

Chien-Shiung Wu College, Southeast University, Nanjing, China
Email: *213213490@seu.edu.cn

How to cite this paper: Zhou, Z.C., Li, J.Y., Lu, S.S. and Lin, Q.Y. (2024) Biomimetic Infiltrating Surface Construction Based on Micro and Nano Structures. *Journal of Materials Science and Chemical Engineering*, **12**, 83-91.
https://doi.org/10.4236/msce.2024.126007

Received: May 8, 2024
Accepted: June 25, 2024
Published: June 28, 2024

Abstract

Microfluidic chips hold significant potential for applications in various fields, such as biological analysis, chemical separation, and drug screening. Here, we draw inspiration from the natural ability of aquatic plants to capture different substances in streams, focusing on the design and fabrication of surfaces with micron and nano-scale structures to mimic the wetting phenomenon observed in nature, thereby achieving the capture and separation of specific substances. This paper reports on the self-assembly of magnetic nanoparticles, the preparation of flexible magnetic nano-chains, and the modification of microfluidic chip surfaces, providing a novel perspective and approach to microfluidic chip technology.

Keywords

Lab-on-a-Chip, Magnetic Nanoparticles, Biosensors, Microfluidic

1. Introduction

Magnetic nanoparticles (MNPs) exhibit unique magnetic, optical, electrical, and chemical properties, rendering them widely applicable in various fields such as molecular imaging [1]-[4], biological separation [5]-[7], and drug delivery [8]-[10]. Various methods for preparing MNPs, including coprecipitation, thermal decomposition, hydrothermal/solvothermal synthesis, and microemulsion [11], can yield magnetic nanostructures such as nanorods, nanowires, and nanocubes.

The exceptional superparamagnetic properties of MNPs significantly enhance

#Co-first authors.
*Corresponding author.
†Second author.
‡Third author.

the efficiency of capturing, transporting, labeling, and detecting biomolecules when combined with microfluidic chips [12]-[14]. Moreover, the amino and carboxyl functionalization properties of MNPs broaden the range of biomarkers available for surface modification [6]. However, current magnetic particles used in biological separation are often in the form of immunomagnetic beads or films, utilized for efficient capture and release of cells or exosomes [14]-[17]. Therefore, constructing smaller, more responsive magnetic nanostructures is essential for advancing research on microfluidic chips for capturing small molecular biomarkers.

Inspired by the natural ability of aquatic plants to capture substances in streams, we developed flexible magnetic nano-chains (FMNCs) and modified them onto the surface of microfluidic chips to achieve biomimetic wettability. The capturing efficiency of FMNCs was evaluated using simple filtration with dithiothreitol as a model biomarker, demonstrating variable capturing efficiency under different magnetic field adjustments.

2. Results and Discussion

2.1. Synthesis of Magnetic Nanoparticles

The size of nanoparticles is typically defined as 1 - 100 nm, and different materials exhibit fundamental nanoscale physical effects at various scales [18]. Additionally, due to quantum size effects, size effects, and surface effects, nanoparticles possess unique optoelectronic properties. Therefore, controlling the size and size distribution of nanoparticles becomes crucial in their preparation [19].

We employed the solvothermal method [20] to prepare nano Fe_3O_4, with $FeCl_3$ as the precursor, poly(sodium 4-styrenesulfonate-co-maleic acid) sodium salt (PSSMA) with a molar ratio of 1:1 as the surfactant, ethylene glycol (EG) and a trace of ascorbic acid (Vc) as the reducing agents, and NaAc and NaOH as the alkali sources to create alkaline conditions. During the experiment, NaAc hydrolysis provided a weakly alkaline environment, and the generated OH^- ions formed complexes with Fe^{3+}, then NaOH was added to create a stronger alkaline environment, making it easier for Fe(III) to be reduced by EG and Vc to generate nano Fe_3O_4. To protect the magnetic nanoparticles from oxidation, tetraethoxysilane (TEOS) was used for encapsulation [21].

Under transmission electron microscopy observation, the $Fe@SiO_2$ particles exhibit regular shapes and uniform sizes (**Figure 1(b)**, **Figure 1(c)**), indicating a relatively ideal synthesis outcome. Furthermore, the $Fe@SiO_2$ particles are uniformly dispersed without aggregation, and the images are clear with sufficient contrast. The thickness of the encapsulating layer is uniform, and the crystal structure is visible without obvious impurities or defects, suggesting good encapsulation quality, which facilitates subsequent chain connection. From the DLS particle size distribution of $Fe@SiO_2$ (**Figure 1(d)**), a sharp single-peak distribution is observed, with a prominent peak representing the primary particle size. Additionally, the peak is relatively narrow and symmetric,

with low fluctuations, indicating a uniform particle size distribution in the sample and stable Brownian motion [22]. There is no significant aggregation or uneven dispersion, which is conducive to the synthesis of uniform flexible nano-chains.

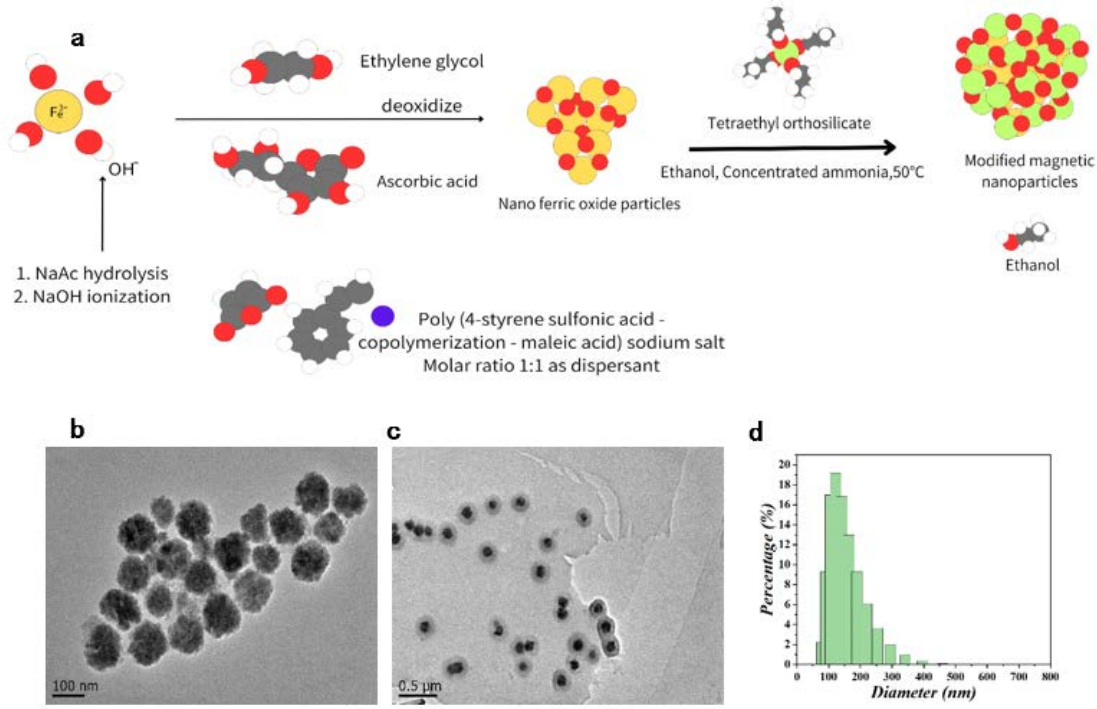

Figure 1. Formation mechanism and structural characterization of magnetic nanoparticles. (a) Mechanism of nano Fe_3O_4 synthesis and silica encapsulation. $FeCl_3$ serves as the iron source, while NaAc and NaOH provide the alkaline environment. PSSMA acts as a dispersant, controlling the particle shape. OH^- ions coordinate with Fe^{3+}, and after ligand decomposition, EG and Vc partially reduce some Fe(III) to Fe(II), forming nano Fe_3O_4. The silica encapsulation process mainly involves the hydrolysis and condensation reactions of TEOS, which can be summarized into three stages: monomer polymerization nucleation, particle growth, and particle connection. (b) TEM imaging of Fe nuclei. (c) TEM imaging of $Fe@SiO_2$. (d) DLS particle size distribution of $Fe@SiO_2$.

2.2. Flexible Magnetic Nanochain Synthesis

For the synthesis of FMNCs, we employed a hydrogen bond-guided template polymerization method[3], utilizing chemical cross-linking to form hydrogels and prepare FMNCs. Using the synthesized $Fe@SiO_2$ as the precursor, HMPP served as the photoinitiator, ethyleneglycol dimethacrylate (EGDMA) as the crosslinker, 2-Hydroxyethyl methacrylate (HEMA) and Acrylic acid (AA) as the monomer for linking. The hydrogen bond-guided template polymerization reaction was conducted under varying lengths of ultraviolet (UV) irradiation. Due to the hydroxyl groups on the surface of silica, hydrogen bonds can form with the photoinitiator. The concentration of crosslinker and monomer near the chain is much higher than in the rest of the solution. Therefore, by controlling the UV irradiation time and magnetic field intensity, polymerization of the monomer can be initiated near the nano-chains, leading to the connection and formation of FMNCs.

The main features of FMNCs include flexibility and magneto responsiveness [23]. Flexibility refers to the ability of the chains to withstand fluid flow without breaking, allowing them to bend and flex freely to effectively trap extracellular vesicles or other substances, serving as a buffer to prevent them from being washed away by the fluid. Magnetoresponsiveness refers to the ability of the chains to respond to magnetic fields, allowing them to exhibit varying degrees of rigidity and angular adjustment under different magnetic field conditions, enabling the chains to capture target substances as needed.

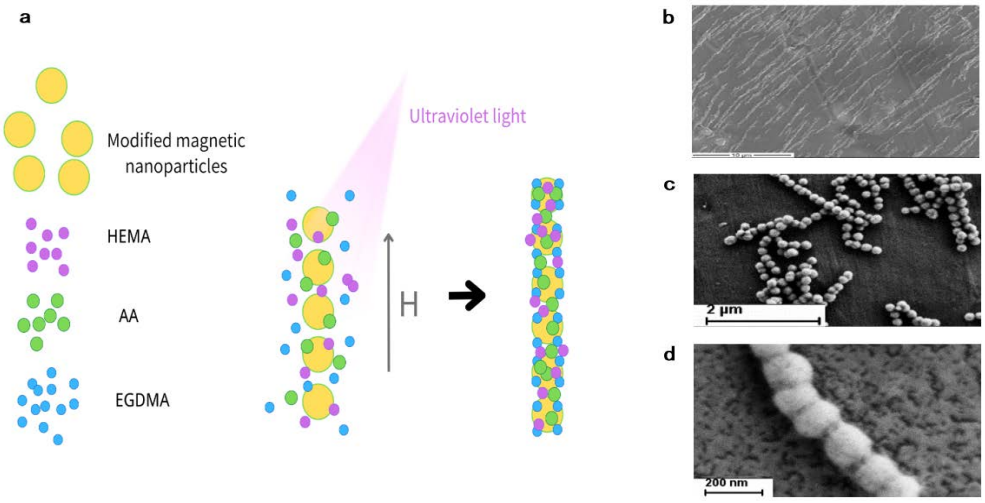

Figure 2. Mechanism and structural characterization of FMNCs synthesis by hydrogen bonding guided template polymerization. (a) Synthesis mechanism of FMNCs. By adjusting the direction and intensity of magnetic field, ultraviolet light intensity, irradiation time and other factors, FMNCs with different properties can be prepared. (b-d) SEM imaging.

After improvements in experimental procedures, continuous chain-like FMNC structures with uniform particle spacing, clear details, and particularly distinct flexible connecting portions can be obtained (**Figures 2(b)-(d)**). This indicates the successful preparation of chains, with flexible connections between nanoparticles [24]. Moreover, there are no apparent defects, fractures, or other abnormal structures observed, indicating the stability and consistency of the preparation process.

2.3. Infiltration Bionic Surface Construction

FMNCs can be connected to surfaces through either direct growth or synthesis immobilization methods. Based on the former approach, a strong magnet is placed at the bottom of the microfluidic chip to generate a stable magnetic field. FMNCs solution is then introduced into the chip and subjected to UV irradiation, resulting in the formation of a small hydrogel filtration device on the surface of polydimethylsiloxane (PDMS). The capturing effect of the surface is verified by capturing bovine serum albumin (BSA), and the content of BSA is quantitatively detected using the biuret method [25].

Due to the adsorption properties of hydrogels on proteins, small proteins can

be filtered at low flow rates. The direction of the magnetic field controls the interception range of the bio-inspired surface. By comparing the data (**Figure 3(c)**), it can be observed that the concentration of Bovine Serum Albumin (BSA) solution with an initial concentration of 12.5 mg/mL, after passing through the microfluidic chip under different magnetic field conditions, becomes 7.7229 mg/mL (vertical magnetic field, FMNCs parallel to the horizontal plane), 5.3741 mg/mL (45˚ magnetic field, FMNCs inclined at 45˚ to the horizontal plane), and 3.8799 mg/mL (parallel magnetic field, FMNCs perpendicular to the horizontal plane), respectively. This confirms the correctness of the inference. Moreover, after modification of FMNCs with antibodies or similar biomolecules, the capturing effect on biomarkers can be significantly enhanced.

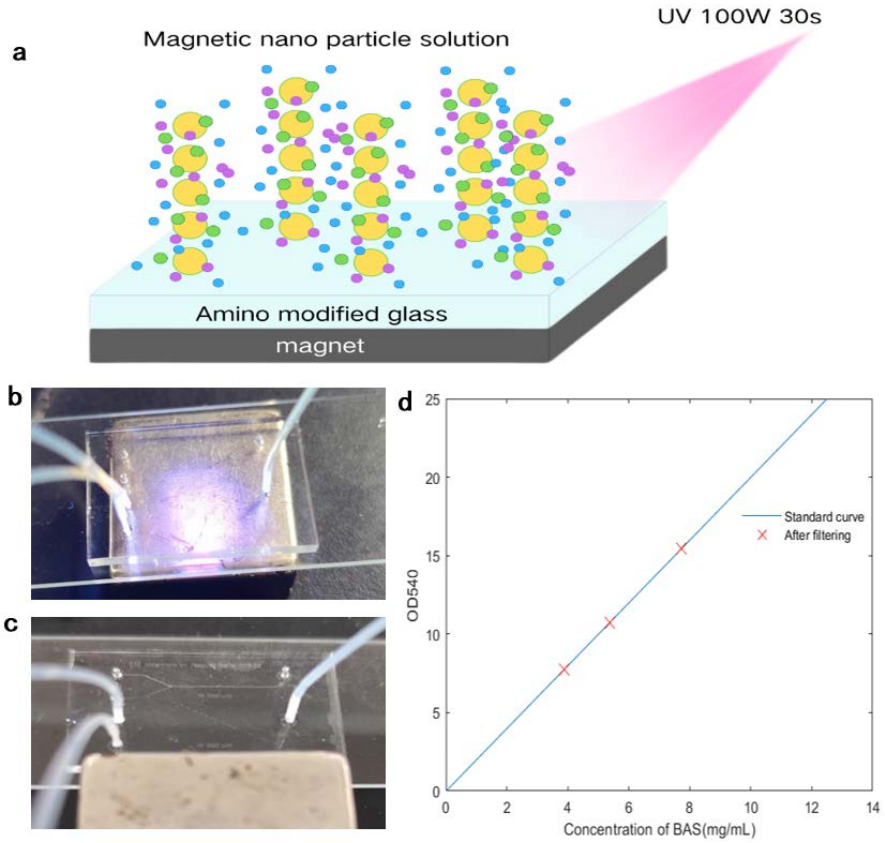

Figure 3. Preparation and feasibility test of infiltrating bionic surface. (a) Preparation mechanism of infiltrating bionic surface. (b) Physical drawings of the preparation of infiltrating bionic surfaces. (c) Parallel magnetic field under BSA through the microfluidic chip. (d) The standard curve of BSA concentration and OD540 and the filtered BSA concentration point. After the original concentration of 12.5 mg /mL BSA flows through the microfluidic chip under different magnetic fields, its concentration becomes 7.7229 mg/mL (vertical magnetic field, FMNCs parallel to the horizontal plane) and 5.3741 mg/mL (45˚ magnetic field), respectively. FMNCs is 45˚ to the horizontal plane), 3.8799 mg/mL (parallel magnetic field, FMNCs is perpendicular to the horizontal plane).

3. Conclusion

In summary, we have successfully prepared bio-inspired FMNCs using the hy-

drogen bond-guided template polymerization method, achieving the construction of an infiltrative biomimetic surface. The capturing efficiency was evaluated using dithiothreitol (DTT) as a detection agent. The flexibility and magnetic controllability of FMNCs allows for rigidness and angular adjustments during the biological separation process under magnetic field control, enabling the chains to capture target substances according to specific needs. Connecting polymer-based magnetic nanoparticles into flexible chains mimics the unique structural characteristics of aquatic plants in nature, which has not been achieved before. By combining the self-assembly of magnetic nanoparticles, the preparation of flexible magnetic nano-chains, and the modification of microfluidic chip surfaces, this study has opened up new avenues for enhancing the functionality of microfluidic devices. The integration of these technologies not only deepens our understanding of micro-scale liquid manipulation but also provides practical solutions for various applications in biomedical diagnostics, chemical analysis, and beyond.

4. Experimental Section

4.1. Nano-Fe_3O_4 Synthesis

Prepare ethylene glycol (EG) by drying it in an oven at 180˚C for 3 hours with 3A molecular sieves to remove moisture. Add 0.26 g of $FeCl_3$, 1.2 g of NaAc, 0.4 g of PSSMA, and 0.004 - 0.0048 g of ascorbic acid (Vc) to 16 mL of dried EG. Then, add 30 μL of deionized water. Ultrasonicate the mixture for 10 minutes and stir at 1500 rpm for 30 minutes to 1 hour until the solution is completely dissolved. Add 0.24 g of NaOH and continue stirring at 1500 rpm until the solution becomes clear and transparent with a yellow-black color. Transfer the fully reacted solution into a lining, and place it into a high-pressure autoclave. Then, perform the following reaction in a muffle furnace: First stage: Ramp up temperature to 30˚C in 15 minutes. Second stage: Maintain temperature at 190˚C for 540 minutes. Third stage: Ramp down temperature to 30˚C in 140 minutes. Finally, maintain the temperature at 30˚C.

4.2. Particle Washing

Cool the muffle furnace to below 60˚C (approximately 40˚C), remove the reaction vessel, and take out the lining. Discard the supernatant and add a 1:1 ethanol-water solution. Wash the particles by stirring and then transfer them to a centrifuge tube. Use a strong magnet to separate the particles, and discard the supernatant once it becomes clear. Repeat the process with another 1:1 ethanol-water solution, mix well, and repeat the washing process at least three times with pure water. After discarding the supernatant, add no more than 12 mL of pure water, mix well, and transfer to a black bottle and seal with a sealing film.

4.3. Fe@SiO_2 Synthesis

Take 12 mL of magnetic particle solution and add 80 mL of ethanol and 4 mL of

ammonia solution. After ultrasonication for about 5 minutes, set up the reaction apparatus on a magnetic stirrer with a water bath heater. Heat the water bath to 50˚C, pour in the solution, and stir for 10 minutes. Then, add TEOS dropwise (approximately 5 μL per 20 seconds) while stirring. Seal the container and stir for 1 hour at 50˚C. Transfer the resulting solution into a centrifuge tube, use a strong magnet to separate the particles, and wash with ethanol 3 - 4 times and with pure water 3 times.

4.4. FMNCs Synthesis

Mix 7.5 mg of Fe@SiO_2, 156 mg of HEMA, 129 mg of AA, 12mg of EGDMA, 3 g of EG, and 1 g of pure water. Add HMPP 10 mg under low light conditions. After vortex shaking, perform UV irradiation under magnetic attraction. By adjusting parameters such as the distance between the UV light and the sample, the distance between the magnet and the sample, the direction and intensity of the magnetic field, UV light intensity, and irradiation time, FMNCs with different properties can be synthesized.

4.5. Surface Mimicking of Wettability for Bionic Surface Construction

Prepare and measure the BSA concentration standard curve.

Take 20 μL of the solution with the same ratio as FMNCs synthesis and inject it into a segment of the conduit to fill the inner wall of the pipeline. Place a magnet at the bottom of the microfluidic chip and expose it to UV light for a certain period to form a hydrogel filtration device. Then, introduce water and ethanol through the conduit to wash away excess impurities. One conduit controls the constant pressure of the gas, while another conduit introduces the test liquid. Utilize a spectrophotometer to measure the protein content of the filtered liquid using the dinitrophenylhydrazine (DNPH) method.

Table 1. BSA standard curve sample configuration.

Sample	Volume			
	BSA (25 mg/mL)	ddH_2O	Biuret A	Biuret B
Standard sample 1	0	1	0.5	0.5
Standard sample 2	0.2	0.8	0.5	0.5
Standard sample 3	0.4	0.6	0.5	0.5
Standard sample 4	0.6	0.4	0.5	0.5
Standard sample 5	0.8	0.2	0.5	0.5
Standard sample 6	1	0	0.5	0.5

Acknowledgements

The author would like to thank the anonymous reviewers for their insightful comments and suggestions that greatly improved the quality of this paper.

Thanks to the teachers, seniors and classmates who helped us during the experiment. This work was supported by the project of the Student Research Training Program for Overseas Students from Chien-Shiung Wu College of Southeast University (NO. 202361055).

Conflicts of Interest

The authors declare no conflicts of interest regarding the publication of this paper.

References

[1] Zhang, C., Liu, T., Gao, J., Su, Y. and Shi, C. (2010) Recent Development and Application of Magnetic Nanoparticles for Cell Labeling and Imaging. *Mini-Reviews in Medicinal Chemistry*, **10**, 194-203. https://doi.org/10.2174/138955710791185073

[2] Kolosnjaj-Tabi, J., Wilhelm, C., Clément, O. and Gazeau, F. (2013) Cell Labeling with Magnetic Nanoparticles: Opportunity for Magnetic Cell Imaging and Cell Manipulation. *Journal of Nanobiotechnology*, **11**, S7. https://doi.org/10.1186/1477-3155-11-s1-s7

[3] Luo, W., Cui, Q., Fang, K., Chen, K., Ma, H. and Guan, J. (2018) Responsive Hydrogel-Based Photonic Nanochains for Microenvironment Sensing and Imaging in Real Time and High Resolution. *Nano Letters*, **20**, 803-811. https://doi.org/10.1021/acs.nanolett.7b04218

[4] Oberdick, S.D., Jordanova, K.V., Lundstrom, J.T., Parigi, G., Poorman, M.E., Zabow, G., *et al.* (2023) Iron Oxide Nanoparticles as Positive T_1 Contrast Agents for Low-Field Magnetic Resonance Imaging at 64 mT. *Scientific Reports*, **13**, Article No. 11520. https://doi.org/10.1038/s41598-023-38222-6

[5] Khizar, S., Ben Halima, H., Ahmad, N.M., Zine, N., Errachid, A. and Elaissari, A. (2020) Magnetic Nanoparticles in Microfluidic and Sensing: From Transport to Detection. *Electrophoresis*, **41**, 1206-1224. https://doi.org/10.1002/elps.201900377

[6] Materón, E.M., Miyazaki, C.M., Carr, O., Joshi, N., Picciani, P.H.S., Dalmaschio, C.J., *et al.* (2021) Magnetic Nanoparticles in Biomedical Applications: A Review. *Applied Surface Science Advances*, **6**, Article ID: 100163. https://doi.org/10.1016/j.apsadv.2021.100163

[7] Zhang, Y., Zhang, F., Song, Y., Shen, X., Bu, F., Su, D., *et al.* (2023) Interfacial Polymerization Produced Magnetic Particles with Nano-Filopodia for Highly Accurate Liquid Biopsy in the PSA Gray Zone. *Advanced Materials*, **35**, Article ID: 2303821. https://doi.org/10.1002/adma.202303821

[8] Ebadi, M., Bullo, S., Buskara, K., Hussein, M.Z., Fakurazi, S. and Pastorin, G. (2020) Release of a Liver Anticancer Drug, Sorafenib from Its PVA/LDH- and PEG/LDH-Coated Iron Oxide Nanoparticles for Drug Delivery Applications. *Scientific Reports*, **10**, Article No. 21521. https://doi.org/10.1038/s41598-020-76504-5

[9] Al-Obaidy, R., Haider, A.J., Al-Musawi, S. and Arsad, N. (2023) Targeted Delivery of Paclitaxel Drug Using Polymer-Coated Magnetic Nanoparticles for Fibrosarcoma Therapy: *In Vitro* and *in Vivo* Studies. *Scientific Reports*, **13**, Article No. 3180. https://doi.org/10.1038/s41598-023-30221-x

[10] Chen, J., Ren, T., Xie, L., Hu, H., Li, X., Maitusong, M., *et al.* (2024) Enhancing Aortic Valve Drug Delivery with PAR2-Targeting Magnetic Nano-Cargoes for Cal-

cification Alleviation. *Nature Communications*, **15**, Article No. 557. https://doi.org/10.1038/s41467-024-44726-0

[11] Monteserín, M., Larumbe, S., Martínez, A.V., Burgui, S. and Francisco Martín, L. (2021) Recent Advances in the Development of Magnetic Nanoparticles for Biomedical Applications. *Journal of Nanoscience and Nanotechnology*, **21**, 2705-2741. https://doi.org/10.1166/jnn.2021.19062

[12] Nam, J., Thaxton, C.S. and Mirkin, C.A. (2003) Nanoparticle-Based Bio-Bar Codes for the Ultrasensitive Detection of Proteins. *Science*, **301**, 1884-1886. https://doi.org/10.1126/science.1088755

[13] Nabaei, V., Chandrawati, R. and Heidari, H. (2018) Magnetic Biosensors: Modelling and Simulation. *Biosensors and Bioelectronics*, **103**, 69-86. https://doi.org/10.1016/j.bios.2017.12.023

[14] Cheng, J., Zhu, N., Zhang, Y., Yu, Y., Kang, K., Yi, Q., *et al.* (2022) Hedgehog-Inspired Immunomagnetic Beads for High-Efficient Capture and Release of Exosomes. *Journal of Materials Chemistry B*, **10**, 4059-4069. https://doi.org/10.1039/d2tb00226d

[15] Gagnon, P., Toh, P. and Lee, J. (2014) High Productivity Purification of Immunoglobulin G Monoclonal Antibodies on Starch-Coated Magnetic Nanoparticles by Steric Exclusion of Polyethylene Glycol. *Journal of Chromatography A*, **1324**, 171-180. https://doi.org/10.1016/j.chroma.2013.11.039

[16] Jauregui, R., Srinivasan, S., Vojtech, L.N., Gammill, H.S., Chiu, D.T., Hladik, F., *et al.* (2018) Temperature-Responsive Magnetic Nanoparticles for Enabling Affinity Separation of Extracellular Vesicles. *ACS Applied Materials & Interfaces*, **10**, 33847-33856. https://doi.org/10.1021/acsami.8b09751

[17] Eivazzadeh-Keihan, R., Bahreinizad, H., Amiri, Z., Aliabadi, H.A.M., Salimi-Bani, M., Nakisa, A., *et al.* (2021) Functionalized Magnetic Nanoparticles for the Separation and Purification of Proteins and Peptides. *TrAC Trends in Analytical Chemistry*, **141**, Article ID: 116291. https://doi.org/10.1016/j.trac.2021.116291

[18] LaConte, L., Nitin, N. and Bao, G. (2005) Magnetic Nanoparticle Probes. *Materials Today*, **8**, 32-38. https://doi.org/10.1016/s1369-7021(05)00893-x

[19] Akbarzadeh, A., Samiei, M. and Davaran, S. (2012) Magnetic Nanoparticles: Preparation, Physical Properties, and Applications in Biomedicine. *Nanoscale Research Letters*, **7**, Article No. 144. https://doi.org/10.1186/1556-276x-7-144

[20] Deng, H., Li, X., Peng, Q., Wang, X., Chen, J. and Li, Y. (2005) Monodisperse Magnetic Single-Crystal Ferrite Microspheres. *Angewandte Chemie International Edition*, **44**, 2782-2785. https://doi.org/10.1002/anie.200462551

[21] Li, Y., Church, J.S., Woodhead, A.L. and Moussa, F. (2010) Preparation and Characterization of Silica Coated Iron Oxide Magnetic Nano-Particles. *Spectrochimica Acta Part A*: *Molecular and Biomolecular Spectroscopy*, **76**, 484-489. https://doi.org/10.1016/j.saa.2010.04.004

[22] Huynh, K. and Partch, C.L. (2015) Analysis of Protein Stability and Ligand Interactions by Thermal Shift Assay. *Current Protocols in Protein Science*, **79**, 28.9.1-28.9.14. https://doi.org/10.1002/0471140864.ps2809s79

[23] Townsend, J., Burtovyy, R., Galabura, Y. and Luzinov, I. (2014) Flexible Chains of Ferromagnetic Nanoparticles. *ACS Nano*, **8**, 6970-6978. https://doi.org/10.1021/nn501787v

[24] Capsoni, M. (2016) On-Surface Self-Assembly and Characterization of a Macromolecular Charge Transfer Complex by Scanning Tunneling Microscopy and Spec-

troscopy. Thesis/Dissertation, University of British Columbia. https://api.semanticscholar.org/CorpusID:139164539

[25] Pokhrel, P., Jha, S. and Giri, B. (2020) Selection of Appropriate Protein Assay Method for a Paper Microfluidics Platform. *Practical Laboratory Medicine*, **21**, e00166. https://doi.org/10.1016/j.plabm.2020.e00166